Clays and Clay Minerals, Vol. 43, No. 2, 196–211, 1995.

DEHYDROXYLATION OF ALUMINOUS GOETHITE: UNIT CELL DIMENSIONS, CRYSTAL SIZE AND SURFACE AREA

H. D. RUAN AND R. J. GILKES

Soil Science and Plant Nutrition, Faculty of Agriculture, University of Western Australia
Nedlands, WA 6907, Australia

Abstract—This work investigates unit cell dimensions, crystal size and specific surface area of aluminous goethite that was progressively dehydroxylated to form hematite. Goethite synthesized from the ferrous system altered to hematite with DTGA maximum increasing from 236° to 273°C for 0 to 30.1 mole % Al-substitution. Unit cell dimensions of goethite and hematite decreased as Al-substitution increased and increased as excess OH increased. The crystallographically equivalent a axis of goethite and c axis of hematite were more sensitive than other axes to the presence of excess structural OH associated with Al-substitution. Specific surface area increased from 147 to 288 m^2/g for goethite and from 171 to 230 m^2/g for hematite as Al-substitution increased. An increase in specific surface area on heating goethite at temperatures between 200° and 240°C is related to a decrease in the size of coherently diffracting domains of goethite crystals and to the development of pore and structural defects associated with the formation of hematite. The decrease in specific surface area for heating temperatures above 240°C is attributed to the growth of hematite crystals by diffusion.

Key Words—Al-substitution, Crystal size, Dehydroxylation, Goethite, Hematite, Specific surface area, Unit cell.

INTRODUCTION

Dehydroxylation of goethite in soil with the formation of hematite may occur in some environments due to natural and managed fires. This alteration is also a component of some manufacturing processes (Perinet and Lafont 1972a, 1972b). The properties of hematite formed by the dehydroxylation of goethite, including Al-substituted goethite, are not well defined and deserve further study. This hematite may contain excess structural OH which mostly affects the unit cell c dimension (Wolska and Schwertmann 1989, Stanjek and Schwertmann 1992). Excess OH also occurs in goethite and mostly strongly affects the unit cell a dimension (Schulze 1984, Schulze and Schwertmann 1984, 1987). These two crystallographic directions are equivalent in that they are perpendicular to the planes of hexagonal close packed O^{2-} anions that are preserved during the topotactic alteration of goethite to hematite (Bernal *et al* 1959).

The dehydroxylation of goethite can be influenced by Al-substitution (Jónás and Solymár 1970, Fey and Dixon 1981), particle size and structural defects (Mackenzie and Berggren 1970). Excess or non-stoichiometric OH may reduce goethite dehydroxylation temperature (Schulze and Schwertmann 1984, Goss 1987). Goethite formed from Fe^{2+} systems usually contains more excess OH and has a lower dehydroxylation temperature than goethite synthesized from Fe^{3+} systems. Hematite formed via the low temperature calcination (e.g., $\leq$300°C) of precursive goethite may inherit excess OH and crystal characteristics of the parent goethite. This paper considers the dehydroxylation of Al-goethite to form Al-hematite. It is part of a study of how Al-substitution and dehydroxylation influence the mineralogical and surface chemical properties of these oxides.

MATERIALS AND METHODS

Al-goethite was synthesized from the ferrous system using a method similar to Fey and Dixon (1981) and Goodman and Lewis (1981). $AlCl_3 \cdot 6H_2O$ and $FeCl_2 \cdot 4H_2O$ were mixed to give [$Al^{3+}/Fe^{2+} + Al^{3+}$] mole percentages equivalent to 0, 10, 20 and 30 mole % Al. Cation concentrations (i.e., $Fe^{2+} + Al^{3+}$) were set to 0.1 M in a total solution volume of 4000 ml. Sodium bicarbonate solution was used to buffer the system at approximately pH 7 during the process of oxidation with about 5 mmole/liter excess of $NaHCO_3$ being present. Air for oxidation was delivered through a sintered glass bubbling tube at 22–25 ml/min. The pH remained at 6.5–6.8 and then rose to about 8.2 at the completion of oxidation. A solution of 0.2 M ammonium oxalate at pH 3.0 was used to extract poorly crystalline compounds from precipitates in the dark, with five consecutive extractions being made at which stage dissolved Fe was at a constant low level (McKeague and Day 1966). The precipitate was washed three times with deionized water and twice with acetone and dried at 110°C in an oven. The dry materials were gently crushed and stored in a desiccator. All subsequent measurements were carried out on the materials remaining after oxalate extraction. Al-substituted hematite was formed by heating sub-samples of Al-substituted goethite in a muffle furnace for one hour at temperatures ranging from 180° to 270°C. Each sub-

sample was heated individually at a selected temperature.

The chemical composition of the goethites was determined by dissolving 10 mg of sample in 20 ml concentrated HCl at 60–80°C. After the solid had completely dissolved, the solution was poured into a 100 ml volumetric flask and made up to the mark with deionized water. The Fe and Al in solution were determined using atomic absorption spectrometry (AAS). An air/acetylene flame was used for Fe and a nitrous oxide/acetylene flame was used for Al. The measured amounts of Al-substitution were 0, 9.7, 19.7 and 30.1 mole % for nominal Al molar contents of 0, 10, 20, and 30 mole % respectively.

X-ray diffraction (XRD) analyses using CuKα radiation were carried out on a computer controlled Sieray modification of a Philips 1050 vertical goniometer with a graphite diffracted beam monochromator. Subsamples of goethite and hematite were taken from the original and heated materials and prepared for XRD by grinding 200 mg of each sample and back filling an aluminum plate holder. 10% by weight of NaCl was added during grinding to provide an internal standard for spacing and line broadening measurements. Scan speed was 0.3° 2θ per min and the step size was 0.01° 2θ. Patterns were run from 10 to 70° 2θ.

The d-spacings (d-values) and the widths at half height (WHH) of XRD reflections were derived from the XRD patterns using the computer programme XPAS (Singh and Gilkes 1992). Unit cell dimensions (UCD) were calculated from d-values using the unit cell parameter regression programme, Crystallographic Least Squares Template (Novak and Colville 1989). The 020, 110, 111 and 151 reflections were used for goethite, and the 102, 110, 204 and 116 reflections for hematite. The 130 reflection for goethite and 104 reflection for hematite could not be used for these calculations because of overlaps of these reflections in those samples which consisted of mixtures of hematite and goethite. Other reflections were not clearly resolved and could not be used for UCD calculation. Mean coherence length (MCL) was calculated from the corrected widths at half height of XRD reflections using the XPAS program. The hematite/(goethite + hematite) XRD intensity ratio was calculated from the ratio of areas under the 110 reflection of goethite and the 102 reflection of hematite; the integrated areas being provided by the XPAS program.

Transmission electron microscopy (TEM) was carried out by depositing a drop of suspension of goethite and hematite dispersed in distilled water on a carbon-coated copper grid to form a film. Micrographs were obtained using a Hitachi HU11B transmission electron microscope.

Differential thermogravimetric analyses (DTGA) and thermogravimetric analyses (TGA) were carried out using a Perkin-Elmer TGS-2 instrument. Approximately 10 mg of sample was heated in flowing air to 620°C at 10°C min^{-1}. Samples were preheated at 110°C for about 10 minutes to remove most adsorbed water. The temperature of dehydroxylation maximum was obtained from the DTGA output and weight lost at particular temperatures was calculated from the TGA curves and assumed to be H_2O. Four replicate DTGA measurements were made for each sample, and the mean values and standard deviations were calculated.

Specific surface area was determined by the BET method (six-point linear plot) using nitrogen adsorption.

RESULTS AND DISCUSSION

Change of the hematite/(goethite + hematite) XRD intensity ratio during dehydroxylation

For goethite samples heated for one hour at various temperatures, the extent of transformation of goethite to hematite increased as temperature increased. This is illustrated by XRD patterns for 9.7 mole% Al-goethite (Figure 1) which show an increase in the extent of transformation of goethite to hematite with increasing temperature in the range 210–250°C. Goethite started to alter to hematite at about 200°C for 0 mole % Al, 210° C for 9.7 and 19.7 mole % Al and 220°C for 30.1 mole % Al-goethites as shown by the changes in the intensity ratio (Figure 2). All samples had completely altered to hematite in one hour for a heating temperature of 260°C, i.e., no residual goethite detected by XRD. Some OH-groups are retained in the structure of hematite formed at these temperatures (Wolska and Schwertmann 1989) and perhaps partly as a consequence coherently diffracting domains are small and crystals are strained so that hematite reflections are broadened as shown in Figure 1.

Temperature of DTGA dehydroxylation maximum and residual water

Temperature of dehydroxylation maximum determined by DTGA increased linearly from 236° to 273°C ($y = 237.3 + 1.21x$, $R^2 = .99$, $p = .01$) with increasing Al-substitution. Values of dehydroxylation temperature cited in the literature include 270°C for natural non-substituted goethite (Anand and Gilkes 1984), 260–280°C (0–9.7 mole % Al) for goethite synthesized from the ferric system (Lim-Nunez 1985) and 243–293°C (0–40 mole % Al) for goethite synthesized from the ferrous system (Fey and Dixon 1981). The slope value of the plot of the temperature of dehydroxylation maximum versus mole % Al is 1.21 for this work, which is close to the values reported in the literature of 1.08 (calculated by the authors from data of Fey and Dixon 1981) and 1.12 (Schulze 1982). It seems that the Al^{3+} ion retains coordinated OH more strongly than Fe^{3+}, possibly due to the higher ionic potential of Al^{3+}. Consequently, the dehydroxylation temperatures of

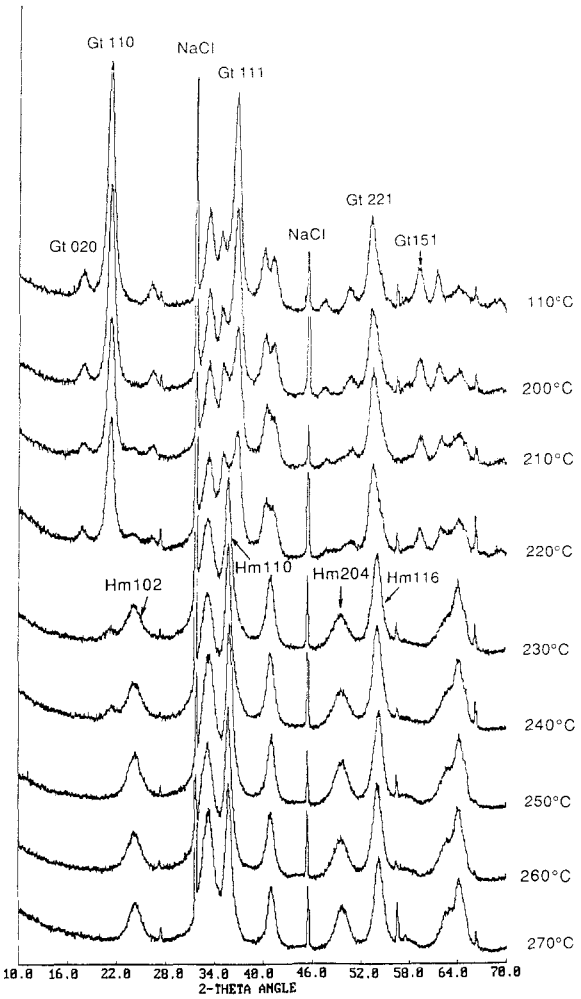

Figure 1. XRD patterns for synthetic 9.7 mole % Al-goethite as affected by heating for one hour at various temperatures.

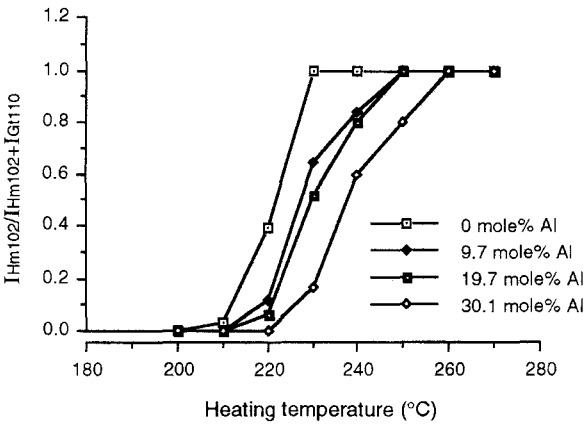

Figure 2. The ratio of intensities of XRD reflections expressed as [hematite(102)/goethite(110) + hematite(102)] for Al-substituted goethite heated at various temperatures.

minum hydroxides are higher than those of corresponding iron hydroxides. For example, the dehydroxylation temperature of boehmite (γ-AlOOH) is 450–500°C, and for isostructural lepidocrocite (γ-FeOOH) is 230–280°C. Similarly, diaspore (α-AlOOH) dehydroxylates at 470–500°C compared with isostructural goethite (α-FeOOH) which dehydroxylates at 230–280°C (Brown 1980). This trend supports the hypothesis that Al ions may specifically retain OH-groups in the structure of Al-hematite when OH associated with Fe has been lost during low temperature dehydroxylation (Fey and Dixon 1981, Schulze 1982, Schulze and Schwertmann 1987). This may also be why greater amounts of chemisorbed surface water and non-stoichiometric OH are associated with synthetic Al-goethite. In this respect it is worth noting that the more hydroxlated oxide of Al (i.e., gibbsite, $Al(OH)_3$) is more common in nature than the less hydrated oxides (boehmite and diaspore AlOOH, corundum Al_2O_3). In contrast the less hydroxylated Fe oxides (goethite FeOOH, hematite Fe_2O_3) are common whereas the most hydroxylated material (bernalite $Fe(OH)_3$) is rare.

TGA results indicated that weight loss due to dehydroxylation increased from 10.5 to 14.6 at DTGA maximum as Al-substitution increased from 0 to 30.1 mole %. Non-stoichiometric OH can remain in the hematite structure after dehydroxylation of Al-goethite giving a compound described as "hydrohematite", α-$Fe_{2-x/3}O_{3-x}OH_x$ (Wolska and Schwertmann 1989). The OH-groups replace oxygen ions in the hematite structure while electroneutrality is preserved by the presence of cation vacancies (Wolska and Schwertmann 1989). The amounts of water lost from Al-goethite formed in the ferrous system are greater than for ideal Al-goethite and Al-goethite synthesized from the ferric system (Schwertmann *et al* 1985). For the present samples, water continued to be released from hematite at temperatures up to 620°C as determined from TGA curves between 110°C and 620°C. Amounts of water lost at 620°C of TGA from previously heated samples (i.e., heated at temperatures between 110° and 270°C) decreased as heating temperature increased (Figure 3). For the samples heated at 110° with Al-substitution from 0 to 30.1 mole %, water lost between 150° and 350°C ranged from 14.2 to 17.4%, represented the dehydroxylation of remaining goethite, whereas water lost at temperatures between 350° and 620°C ranged from 1.4 to 2.9%, presumably represented OH that had persisted in hematite.

Unit cell dimensions of Al-goethite

Previous studies have shown that unit cell parameters of goethite decrease as Al-substitution increases (Thiel 1963, Lewis and Schwertmann 1979, Schulze 1984, Schulze and Schwertmann 1984, 1987, Fazey *et al* 1991), as was also observed in this study (Figure 4). For b and c unit cell parameters, similar but not iden-

https://doi.org/10.1346/CCMN.1995.0430207 Published online by Cambridge University Press

tical changes in size with mole % Al occurred for Al-goethites heated at various temperatures, but there were quite different changes for the a parameter (Figure 4). These changes are best discussed by reference to the slope (●) and intercept (▲) values calculated from the straight lines ($R^2 > .97$, $p < .05$) of Figure 4 as is shown in Figure 5. The intercept values (i.e., the values for 0 mole% Al-goethite heated at various temperatures) of plots of the a unit cell dimension of goethite versus mole % Al decreased systematically by 0.18% as heating temperature increased from 110° to 210°C (Figure 5a). Intercept values for the b unit cell dimension decreased by 0.07% between 110° and 190°C and then increased to the original value at 200°C (Figure 5b). The c dimension decreased by 0.10% on heating at 200°C (Figure 5c). For non-substituted goethite, the influence of excess OH is greatest on the a axis dimension with the intercept value of the line for a being more sensitive than for b and c (Schulze and Schwertmann 1984).

The slopes of lines relating unit cell dimension to Al-substitution for goethite heated to different temperatures (i.e., rate of decrease of unit cell dimension with increasing Al-substitution) shown in the plots of Figure 4 increased in magnitude with increasing temperature (Figures 5e–5g) which reflects a decreasing effect of excess OH and thus the relatively increasing effect of Al-substitution on unit cell size with increasing temperature. The increases in slope value of this line as a proportion of unit cell dimension (i.e., Δslope/UCD) from 110° to 210°C were about 0.26×10^{-4}, 0.45×10^{-4} and 0.92×10^{-4} (mole % Al)$^{-1}$ for the a, b and c axes, respectively. These are large changes in slope; evidently the relationships for all unit cell dimensions are sensitive to the presence of non-stoichiometric OH-groups in the structure of Al-goethite with the c dimension being most sensitive.

The intercept and slope values in Figure 5 for the samples heated at 210°C can be compared with published data and a Vegard line based on JCPDS (1983) cards 29–713 for goethite and 5–355 for diaspore. The intercept values for Al-free goethite in the present study (a = 4.6265 Å, b = 9.9391 Å, c = 3.0269 Å), are quite close to the values reported by Schulze (1982, a = 4.632 Å, b = 9.940 Å, c = 3.024 Å) for goethite synthesized from the ferrous system, and by Jónás and Solymár (1970, a = 4.621 Å, b = 9.939 Å, c = 3.024 Å) for goethite synthesized from the ferric system at 40–50°C. The a and c values are considerably larger than for JCPDS card 29–713 (a = 4.608 Å, c = 3.0215 Å) while the b value is smaller (b = 9.957 Å). The magnitude of the slope value for the relationship for the unit cell c dimension versus mole % Al for 210°C heated goethite in the present study ($c = -16 \times 10^{-4}$) was similar to that of the Vegard line based on JCPDS data ($c = -18 \times 10^{-4}$) whereas the magnitude of slope values for a (-6.4×10^{-4}) and b (-33×10^{-4}) were much

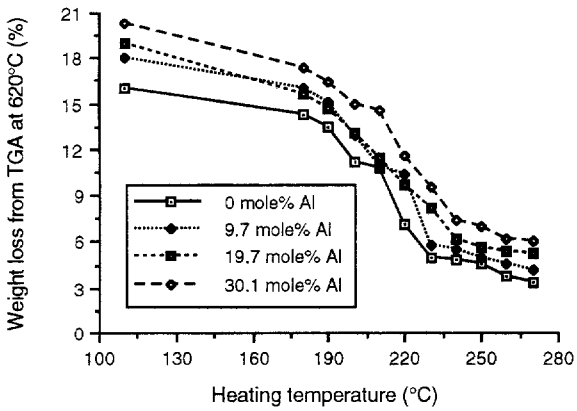

Figure 3. Total weight loss at temperatures between 110° and 620°C from TGA curves versus heating temperature for Al-goethites.

smaller than for the Vegard lines for a (-20×10^{-4}) and b (-53×10^{-4}), respectively derived from JCPDS data.

Unit cell volume (UCV) decreased linearly ($R^2 > .97$, $p < .05$) with the increase in Al-substitution (Figure 4d) and also decreased systematically with heating temperature (intercept values in Figure 5d). The slope values for UCV increased in magnitude from 0.116 to 0.137 (Å^3/mole % Al) with increasing temperature showing that loss of excess OH makes the UCV relationship trend (Figure 5h) towards the ideal Vegard relationship (slope value for JCPDS data is 0.204). A similar trend has been reported by Taylor and Schwertmann (1978), for Al-substitution ranging from 5.4 to 23.5 mole %.

Evidently, the departures of unit cell parameters from values for the ideal Vegard relationships are at least partly due to the presence of excess OH. By comparing goethites synthesized at 25°C from the ferric system with those synthesized at 70°C, Schulze and Schwertmann (1987) found that the unit cell a and c dimensions for the samples synthesized at 25°C were 0.006–0.014 Å and 0.0037 Å larger respectively than for the samples synthesized at 70°C. The b dimension was similar for samples synthesized at both temperatures. The larger a and c dimensions indicate that the goethites synthesized at 25°C contain more structural defects and those defects are believed to be associated with the structural OH content which increases with increasing Al-substitution. Schwertmann *et al* (1985) reported that the a dimension is about 0.02 Å larger for goethites synthesized between 4° and 30°C than for goethites synthesized between 50° and 80°C. Schulze and Schwertmann (1984) indicated that Δa, defined as the observed a dimension minus the a dimension predicted by the ideal Vegard relationship, is related to structural defects associated with an increase in OH in the goethite structure. They also found that goethite synthesized in 2 M KOH had larger Δa values than goethite synthe-

https://doi.org/10.1346/CCMN.1995.0430207 Published online by Cambridge University Press

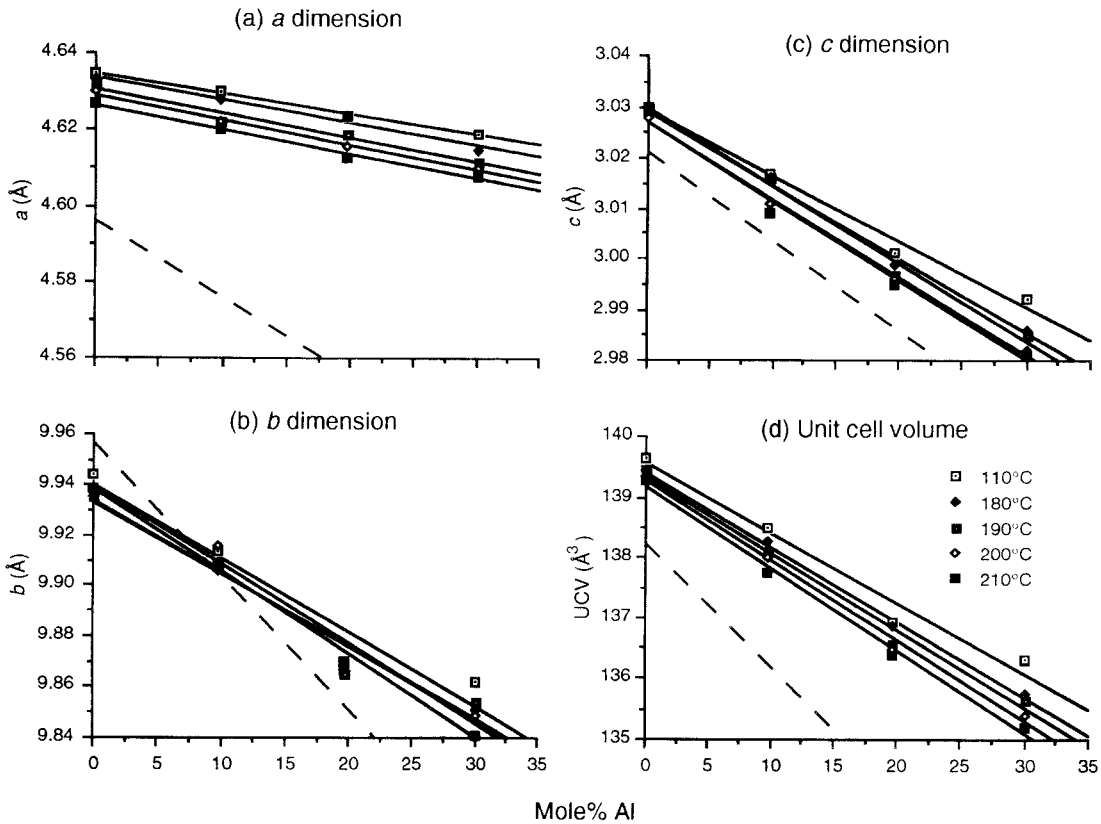

Figure 4. Unit cell dimensions (a, b, c) and unit cell volume of goethite as affected by Al-substitution and heating; R^2 values for these relationships are between .972 ($p < .05$) and .999 ($p < .01$). The broken lines are the ideal Vegard lines.

sized in 0.3–0.4 M KOH, concluding that the high OH concentration in the synthesis solution induces excess OH into the goethite structure, resulting in higher Δa values.

The influence of excess OH on unit cell parameters becomes more complex when goethite also contains Al as both constituents affect these parameters. Figure 6 shows goethite unit cell dimensions plotted against the total weight loss (assumed H_2O loss, TGA data) between 110° and 620°C for Al-goethites that had been previously heated at various temperatures below the dehydroxylation temperature (i.e., ≤210°C). There are good, nearly linear, relationships of unit cell a and c parameters and UCV with excess water but mostly no systematic change for the b parameter. When the slopes of these regression lines are expressed as percentage changes of the unit cell dimensions (Table 1), it is evident that values of slope increase with Al-substitution and that the a and c dimensions are more sensitive to water content (i.e., mean slope values of about 0.034) than the b dimension (i.e., mean slope value of 0.009) with the exception of the highest level of Al-substitution (i.e., 30.1 mole %) where the b axis was sensitive to water content (Figure 6b). Unit cell volume increased with increasing water content for all four goethites (Figure 6d). For each heating temperature, water content increased with increasing Al-substitution with the combined effect being a decrease in unit cell volume as Al content increased (Figure 6d). Stepwise linear regression analysis was used to develop the relationships of unit cell parameters with Al-substitution and water content. The predictive equations are expressed on a percentage change basis:

$$a\% = 100 - (0.017 \pm 0.001)\ \text{mole \% Al} + (0.033 \pm 0.004)\ \text{WL\%} \quad (R^2 = .96),$$

$$b\% = 100 - (0.031 \pm 0.002)\ \text{mole \% Al} + (0.010 \pm 0.007\ \text{WL\%} \quad (R^2 = .96),$$

$$c\% = 100 - (0.053 \pm 0.001)\ \text{mole \% Al} + (0.036 \pm 0.007)\ \text{WL\%} \quad (R^2 = .99),$$

$$UCV\% = 100 - (0.102 \pm 0.003)\ \text{mole \% Al} + (0.078 \pm 0.012)\ \text{WL\%} \quad (R^2 = .99)$$

https://doi.org/10.1346/CCMN.1995.0430207 Published online by Cambridge University Press

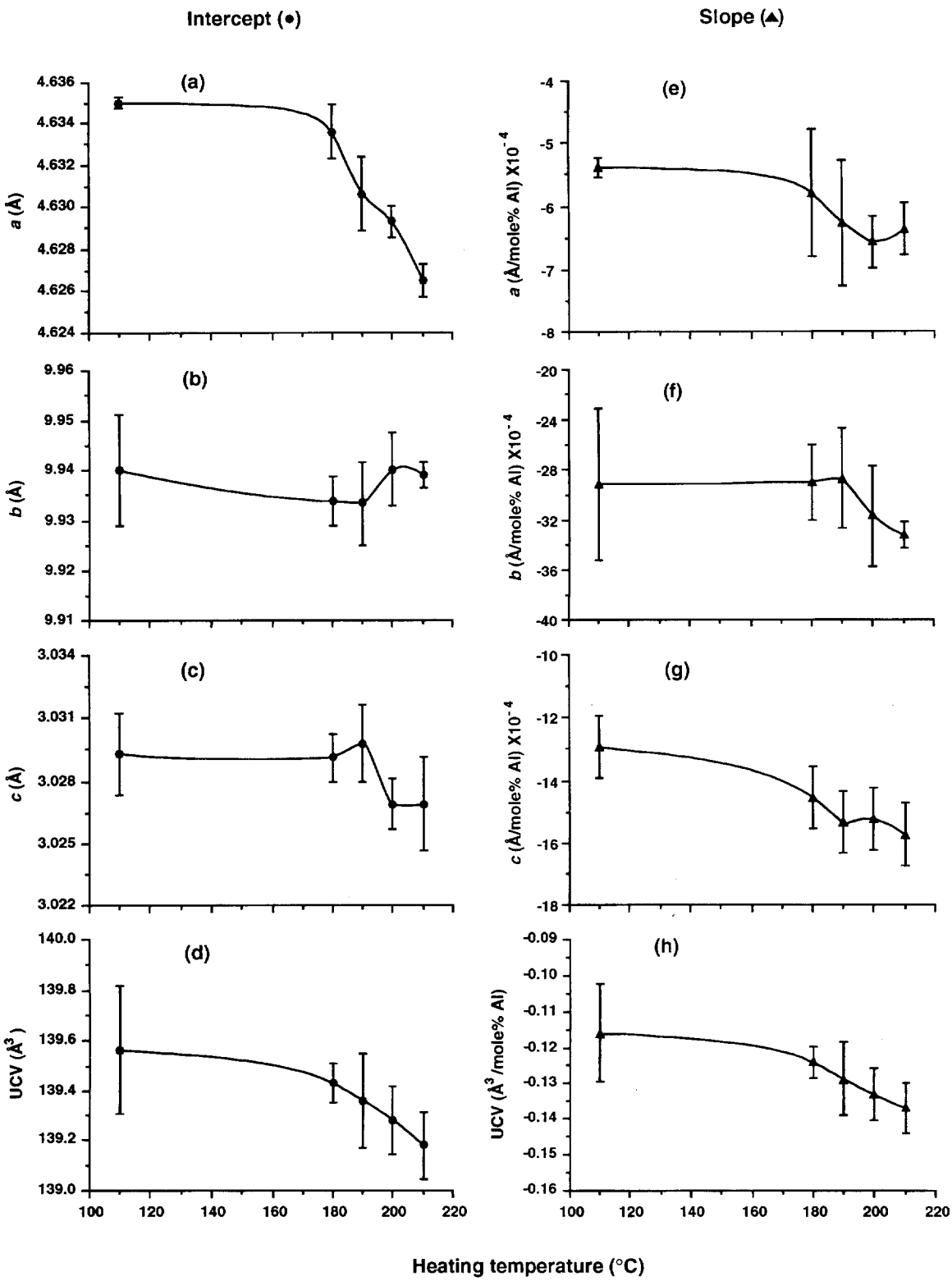

Figure 5. Intercept and slope values for straight lines relating unit cell dimensions and unit cell volume of goethite to Al-substitution plotted against heating temperature (110–210°C), (a) (e) a dimension, (b) (f) b dimension, (c) (g) c dimension and (d) (h) unit cell volume.

https://doi.org/10.1346/CCMN.1995.0430207 Published online by Cambridge University Press

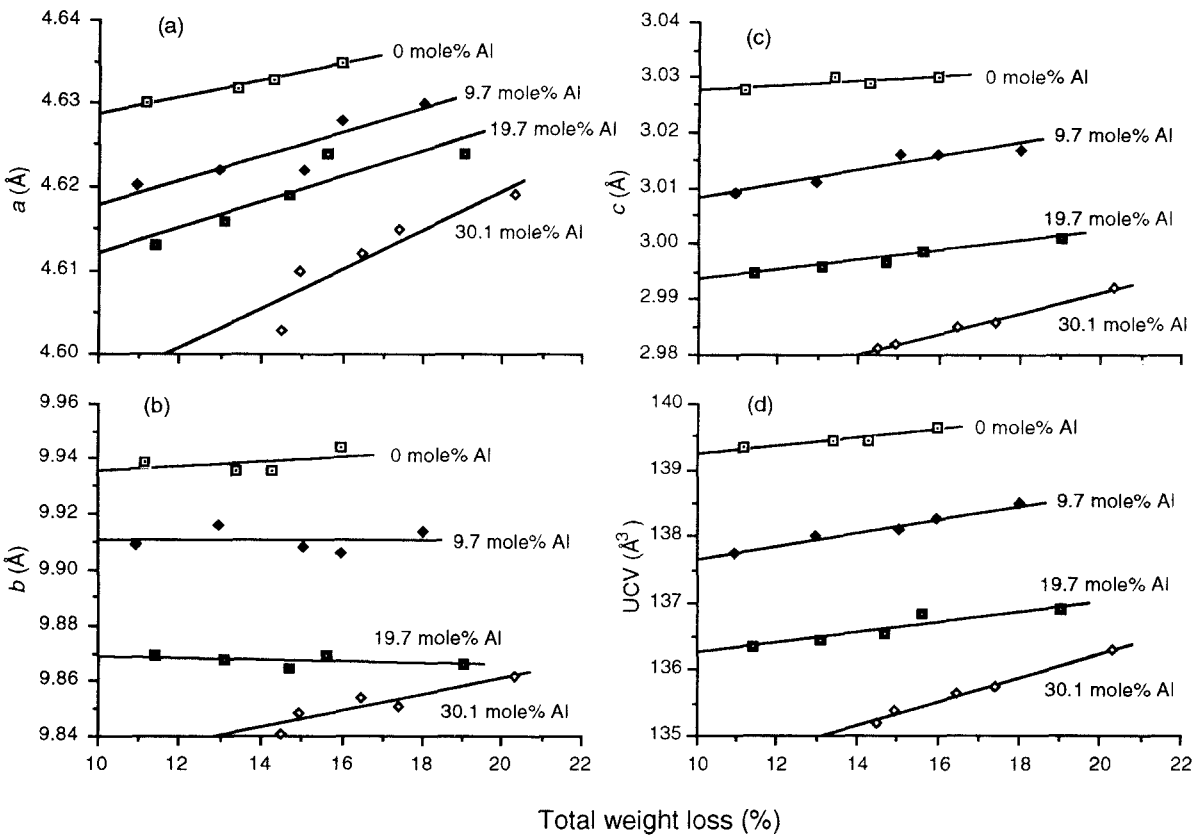

Figure 6. Unit cell dimensions a (a), b (b), c (c) and unit cell volume (d) of goethite heated at various temperatures up to the onset of hematite formation (200°C for 0 mole% Al and 210°C for others) plotted against total weight loss from TGA at 620°C. R^2 values and errors as in Table 1.

where WL% is the percentage of weight loss. Note the opposite effects of Al (negative coefficients) and excess water (positive coefficients) on unit cell dimensions. These results should be assessed by consideration of the structure of goethite which is based on the hexagonal close packing of oxygen atoms with 6-fold coordinated Fe atoms occupying octahedral positions. The Fe atoms are arranged in double row to form what can be described as double chains of octahedra which run the length of the c axis. Within the double chains in the b-c plane, all bonds are covalent with each octahedron sharing four of its edges with neighbouring octahedra. In contrast, bonding between double chains consists of relatively weak H-bonding directed through apical oxygen ions directed along the a axis (Francombe and Rooksby 1959, Schulze 1984). Thus, stacking of double chains along the a axis can be easily disrupted and this consequently induces structural defects, i.e., excess OH incorporated into the goethite structure during crystal growth (Fey and Dixon 1981, Schulze and Schwertmann 1984, 1987, Schwertmann *et al* 1985). For crystal growth of goethite, Lewis and Schwertmann (1980) indicate that the smallest thickness of crystals along the crystallographic a axis develops its final size at an early stage of growth whereas crystal growth along b and c axes may continue. The faster the crystal growth along the a axis, the more structural defects are induced and presumably more excess OH is incorporated.

According to the model proposed by Schulze (1982), the amount of nonstoichiometric OH incorporated into the goethite structure can be explained by one Fe or Al ion being replaced by three H ions. The proportion of Fe and Al ions replaced by three H ions is expressed by the formula,

$$\alpha\text{-}Fe_{1-y}Al_y)_{1-x/3}O_{1-x}(OH)_{1+x}$$

where x represents the fraction of Fe and Al ions replaced by three H ions, and y is the mole fraction of Al-substitution. This replacement is believed to occur mainly along the a axis (Schulze 1982) and may explain why the a dimension of non Al-substituted goethite is most sensitive to structural OH.

Unit cell dimensions of Al-hematite

The effect of Al-substitution on the unit cell dimensions of hematite produced by the dehydroxylation of goethite was similar to that for goethite. Figure 7 shows

https://doi.org/10.1346/CCMN.1995.0430207 Published online by Cambridge University Press

Table 1. Percentage change in slope for unit cell dimensions versus total weight loss (TGA, 110–620°C) for goethite and hematite.

			Slope parameter			
	UCD[1]	Mole % AL	Slope	Δslope (%)[2]	Mean (%)	R^2
Gt	*a*	0	0.00103 ± 0.0001	0.022		0.992**
(110–210°C)		9.7	0.00145 ± 0.0004	0.031		0.828*
		19.7	0.00154 ± 0.0004	0.033		0.824*
		30.1	0.00236 ± 0.0006	0.051		0.833*
					0.034 ± 0.0061	
	b	0	0.00086 ± 0.0012	0.0087		0.209
		9.7	0.00003 ± 0.0009	0.0003		0.000
		19.7	−0.00028 ± 0.0004	−0.0028		0.138
		30.1	0.00301 ± 0.0008	0.0306		0.828*
					0.009 ± 0.0075	
	c	0	0.00037 ± 0.0002	0.012		0.613
		9.7	0.00125 ± 0.0002	0.042		0.908*
		19.7	0.00083 ± 0.0001	0.028		0.963**
		30.1	0.00187 ± 0.0001	0.063		0.996***
					0.036 ± 0.0108	
	UCV	0	0.0603 ± 0.0182	0.044		0.847
		9.7	0.1008 ± 0.0072	0.074		0.986***
		19.7	0.0795 ± 0.0193	0.059		0.850*
		30.1	0.1805 ± 0.0142	0.136		0.982**
					0.078 ± 0.0202	
Hm	*a*	0	0.00281 ± 0.0005	0.056		0.912*
(230–270°C for		9.7	0.00355 ± 0.0008	0.071		0.953*
0 mole % Al and		19.7	0.00670 ± 0.0004	0.134		0.996*
250–270°C for		30.1	0.00189 ± 0.0007	0.038		0.887
9.7, 19.7 and					0.075 ± 0.0209	
30.1 mole % Al)						
	c	0	0.01390 ± 0.0031	0.101		0.873*
		9.7	0.01677 ± 0.0037	0.122		0.954
		19.7	0.05309 ± 0.0402	0.388		0.636
		30.1	0.01699 ± 0.0061	0.124		0.887
					0.184 ± 0.0683	
	UCV	0	0.6433 ± 0.1077	0.214		0.922**
		9.7	0.6916 ± 0.1700	0.233		0.943
		19.7	1.6807 ± 1.1995	0.582		0.633
		30.1	0.5921 ± 0.2103	0.203		0.888
					0.381 ± 0.0915	

[1] UCD is unit cell dimensions derived from least squared calculation and UCV is unit cell volume.
[2] Percentage change of slope ((ΔÅ/Å/Δ weight loss) × 100) based on unit cell dimensions calculated from Figures 6 and 9.
*$p < 0.05$, **$p < 0.01$ and ***$p < 0.001$, respectively. R^2 are taken from the regression lines of Figure 6 for goethite and of Figure 9 for hematite.

that unit cell dimensions a and c decreased linearly as Al-substitution increased ($R^2 > .98$, $p < .01$). The a and c dimensions of hematite also decreased with heating temperature (Figure 7). Intercept values for 0 mole % Al-hematite derived from plots of a and c dimensions versus Al-substitution (i.e., Figure 7) decreased systematically with heating temperature (Figures 8a and 8b). The a dimension decreased by 0.13% and the c dimension decreased by 0.18% between 230° and 270°C. These % decreases are similar to those reported by Stanjek and Schwertmann (1992) who found that values of a and c dimensions decreased from 5.042 to 5.033 Å (about 0.18%) and from 13.76 to 13.73 Å (about 0.22%) respectively, as synthesis temperature increased from 40° to 997°C for the 0–18 mole % Al-substituted hematites. Unit cell parameters for a disordered hematite-like phase transformed from goethite between 250° and 350°C were approximately 0.3% larger than those for well crystallized hematite (Brown 1980). The relatively small decrease in the intercept values for the c dimension of hematite (i.e., value for no Al-substitution) with heating temperature compared with the Al-substituted hematites (Figure 7b) indicates that relatively less water was present in non-substituted hematite than in Al-substituted hematite. The magnitude of the change in slope for experimental lines calculated for plots of the a dimension versus mole% Al (Figure 7) decreased by 8% over the heating temperature range 230–270°C (Figure 8d). The magnitude of the change in slope for the c dimension of hematite increased considerably (316%) (Figure 8e) over this temperature range; clearly the c dimension is much

https://doi.org/10.1346/CCMN.1995.0430207 Published online by Cambridge University Press

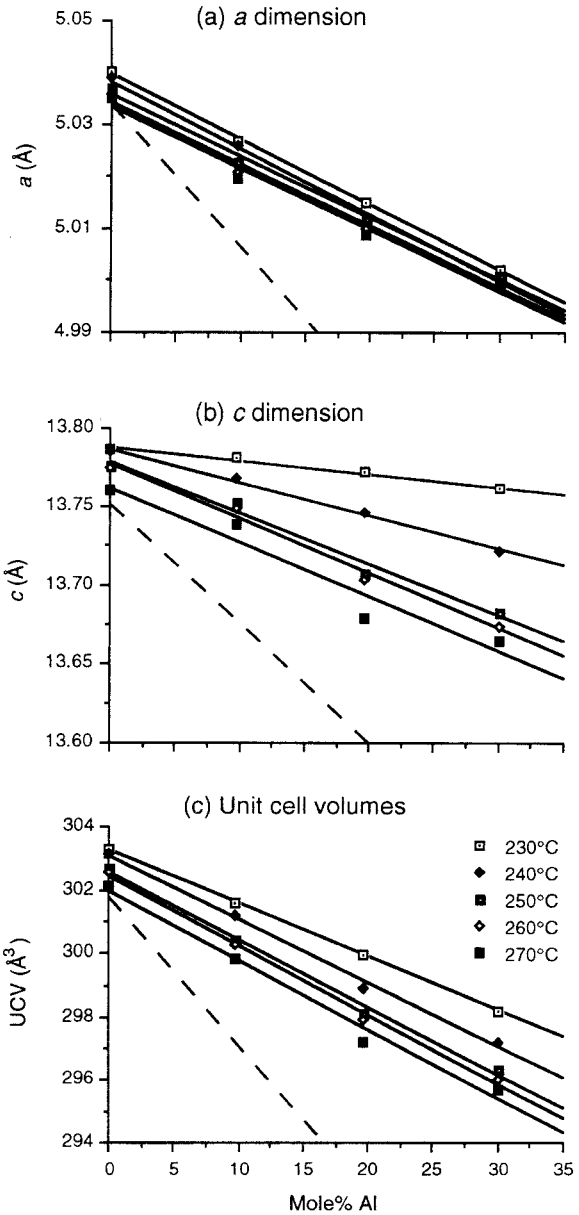

Figure 7. Unit cell dimensions (a, c) and unit cell volume of hematite as affected by Al-substitution and heating; R^2 values are .980–.999 ($p < .01$). The broken lines are the ideal Vegard lines.

more sensitive than the a dimension to the presence of water in the hematite structure. The great sensitivity of the c dimension to heating probably reflects the presence of OH ions in planes parallel to (001), the effect being greater for high Al hematite. This behaviour of the c dimension may not be related only to the presence of OH but also to the migration of cations and rearrangement of oxygen packing, especially over the temperature range of dehydroxylation used in this study. The increase in the c dimension may reflect initial development of the hematite structure along the c direction, comparing with very small hematite domains as indicated by peak broadening. Stanjek and Schwertmann (1992) showed that the relationship of the c dimension to Al content is poorer than for the a dimension. In their work, the deviation of the c dimension (Δc) from the value for the ideal structure was much better related to water content than was Δa.

A comparison of the lines for unit cell parameters versus Al content for Al-hematite for the present study with values of Vegard line based on standard JCPDS (1983) cards 13–534 for hematite and 10–173 for corundum shows that Al-hematite formed at 270°C had a larger c dimension (13.763 Å) than the standard (13.752 Å) whereas the a dimension (5.034 Å) was identical to the value for the standard hematite (5.034 Å). Values of slope of -1.2×10^{-3} and -3.5×10^{-3} (Å/mole % Al) for lines for the a and c dimensions respectively for heating temperatures of 260° and 270°C were smaller in magnitude than those of Vegard lines of -2.8×10^{-3} and -7.6×10^{-3} respectively calculated from JCPDS values. However, the value of slope for the a dimension was similar to that for Al-hematite synthesized via Al-ferrihydrite precursor (-1.5×10^{-3}) (Schwertmann *et al* 1979) and for Al-hematite formed by the dehydroxylation of Al-goethite (-1.6×10^{-3}) (DeGrave *et al* 1982). Wells *et al* (1989) obtained a slope value of -5.7×10^{-3} for the c dimension of hematite formed by the dehydroxylation of synthetic goethite at 350°C, which was larger than the value of -3.5×10^{-3} at 260–270°C for this study but both values were less than the slope value of the Vegard line derived from JCPDS data (-7.6×10^{-3}). Schwertmann *et al* (1979) and DeGrave *et al* (1982) found no systematic trend and reported a scattering of values for the slope for the c dimension, while Stanjek and Schwertmann (1992) reported that the regression lines for the c dimension versus mole % Al varied irregularly as affected by synthesis temperature. The regular increase in magnitude of slope value for the c dimension with increasing temperature is illustrated in Figures 7b and 8e. The smaller magnitude of slope of the c dimension for hematite formed at lower temperatures (i.e., <270°C) is presumably due to excess OH remaining in hematite structure in positions parallel to (001) (Wolska and Schwertmann 1989, Stanjek and Schwertmann 1992), thereby reducing the contracting effect of Al on the unit cell c dimension. As would be anticipated, unit cell volume (UCV) shows a similar trend with Al-substitution to that shown by the a and c unit cell parameters (Figure 7c). The intercepts and slopes of the regression line which are shown in Figures 8c and 8f, demonstrate that the UCV intercept decreased systematically with heating temperature indicating that structural OH retained in the hematite structure is progressively released with increasing temperature. The magnitude of slope values for the plot

https://doi.org/10.1346/CCMN.1995.0430207 Published online by Cambridge University Press

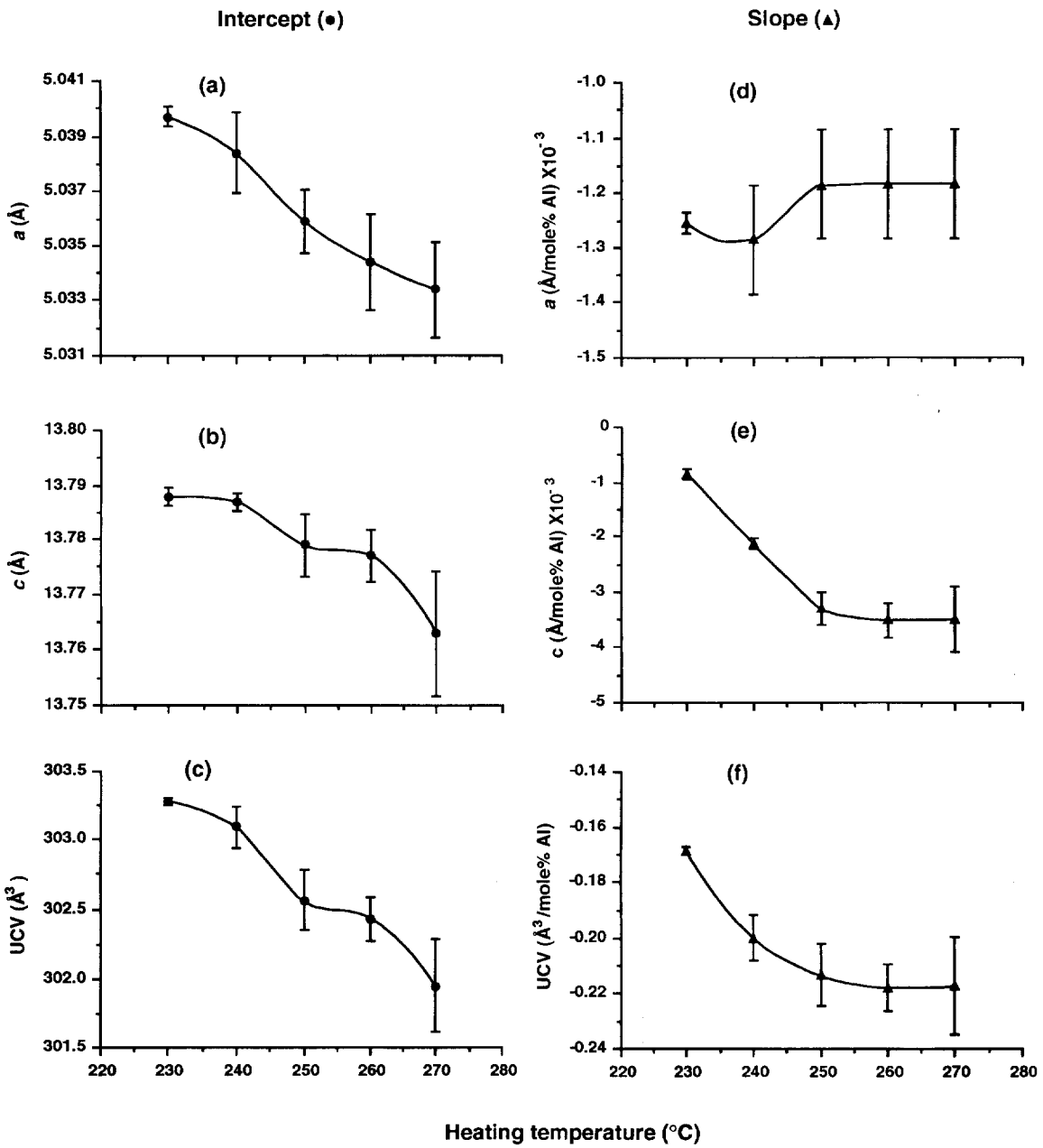

Figure 8. Intercept and slope values for straight lines relating unit cell dimensions and unit cell volume of hematite to Al-substitution plotted against heating temperature (230–270°C); (a) (d) a dimension, (b) (e) c dimension and (c) (f) unit cell volume.

of UCV versus mole % Al increased exponentially with temperature reaching a constant value at 260°C (Figure 8f) as did the c axis slope value (Figure 8e).

It therefore seems probable that the changes in unit cell dimensions of Al-hematite due to heating are a consequence of structural OH that is lost as water and an increasing influence of Al within the hematite structure. Figure 9 shows that for each specimen heated at various temperatures (230–270°C) there are linear relationships between water loss from hematite at 620°C of TGA (total weight loss) and the a and c dimensions. Because of the need to avoid water loss from any goethite present in samples, these data are for specimens that contained only hematite so that the larger unit cell parameters of hematite shown in Figure 7 do not appear in this graph. The close linear relationships indicate that unit cell dimensions provide an indication of the OH in hematite. Table 1 expresses the slopes of

https://doi.org/10.1346/CCMN.1995.0430207 Published online by Cambridge University Press

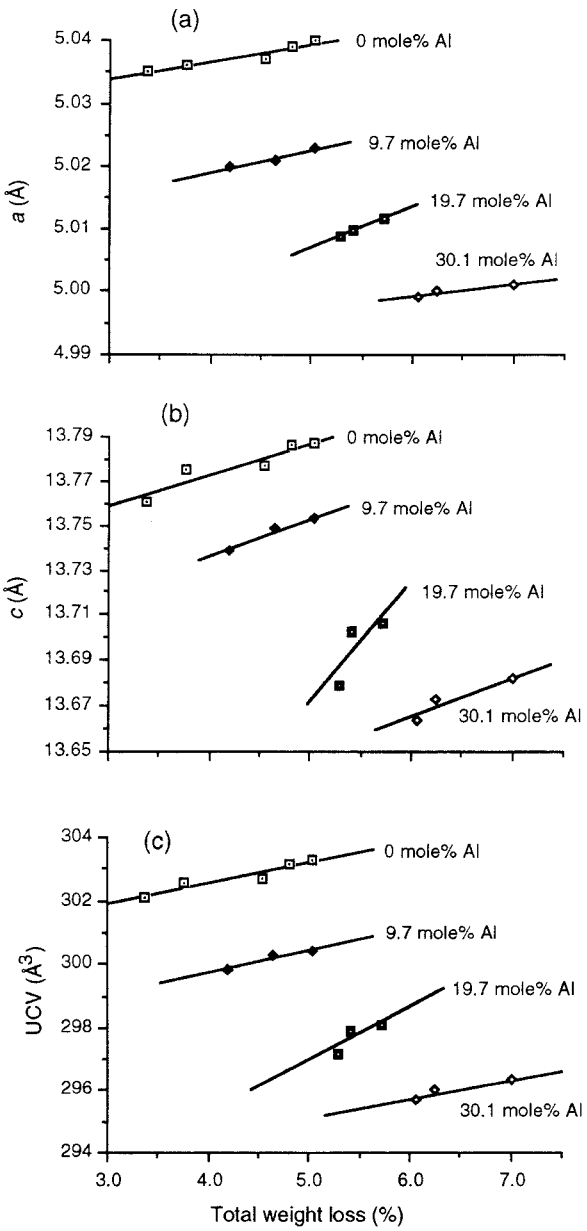

Figure 9. Unit cell dimensions a (a) and c (b) and unit cell volume (c) of hematite produced by dehydroxylation of goethite at various temperatures plotted against total weight loss from TGA at 620°C. R^2 values and errors as in Table 1.

experimental lines in Figure 9 on a percentage change basis. The c axis is about twice as sensitive to OH content (mean value 0.184) as the a axis (0.075) and changes to a and c unit cell dimensions for 19.7 mole % Al hematite are more sensitive to OH content than for other levels of Al-substitution (Table 1). Stanjek and Schwertmann (1992) concluded that some OH remained in the crystal structure of hematite up to approximately 1000°C and this conclusion is supported by other work (Gregg and Hill 1953, Okamoto *et al* 1967, Wolska 1981, Wolska and Szajda 1985). The major differences in unit cell dimensions of the present samples shown in Figure 9, however, are due to differences in Al substitution with relatively less difference being due to excess OH content.

The equations relating unit cell parameters for hematite to mole % Al and total weight loss (WL) were derived by stepwise linear regression analysis and converted to a % basis, are as follows:

$$a\% = 100 - (0.030 \pm 0.002)\ \text{mole \% Al} + (0.074 \pm 0.016)\ \text{WL\%} \quad (R^2 = .99),$$

$$c\% = 100 - (0.034 \pm 0.003)\ \text{mole \% Al} + (0.109 \pm 0.036)\ \text{WL\%} \quad (R^2 = .98),$$

$$UCV\% = 100 - (0.094 \pm 0.004)\ \text{mole \% Al} + (0.252 \pm 0.048)\ \text{WL\%} \quad (R^2 = .99)$$

The c dimension of hematite is more sensitive to structural OH than is the a dimension with a and c dimensions being almost equally sensitive to Al-substitution.

There is a precise crystallographic relationship between the orthorhombic structure of goethite and the hexagonal structure of hematite during the thermal transformation of goethite to hematite. The [100], [010] and [001] directions in the orthorhombic structure become, respectively, the [001], [010] and [210] directions in the hexagonal structure (Brown 1980). Water molecules (as hydroxyl groups) can simply be removed in strips running parallel to the c axis of goethite and some of the Fe and Al atoms are rearranged in the octahedral interstices (Francombe and Rooksby 1959). The mechanism of hematite crystal transformation from goethite is essentially a nucleation process (Watari *et al* 1983). The rearrangement of Fe and Al results in nucleation and associated diffusion, creating voids parallel to the (100) plane of goethite which is the (001) plane of hematite, enabling the escape of water vapour (Naono and Fujiwara 1980, Rendon *et al* 1983). As a result, the unit cell a dimension for goethite (Schulze 1984, Schulze and Schwertmann 1984) and the c dimension for hematite (Stanjek and Schwertmann 1992) are relatively more sensitive to the presence of structural OH.

Crystal size and shape

Transmission electron micrographs of the oxides show that the particles are micro-crystalline, anhedral and decrease in size with increasing Al-substitution for both goethite and hematite (Figure 10). Particles of nonsubstituted goethite have a lath-like crystal shape,

https://doi.org/10.1346/CCMN.1995.0430207 Published online by Cambridge University Press

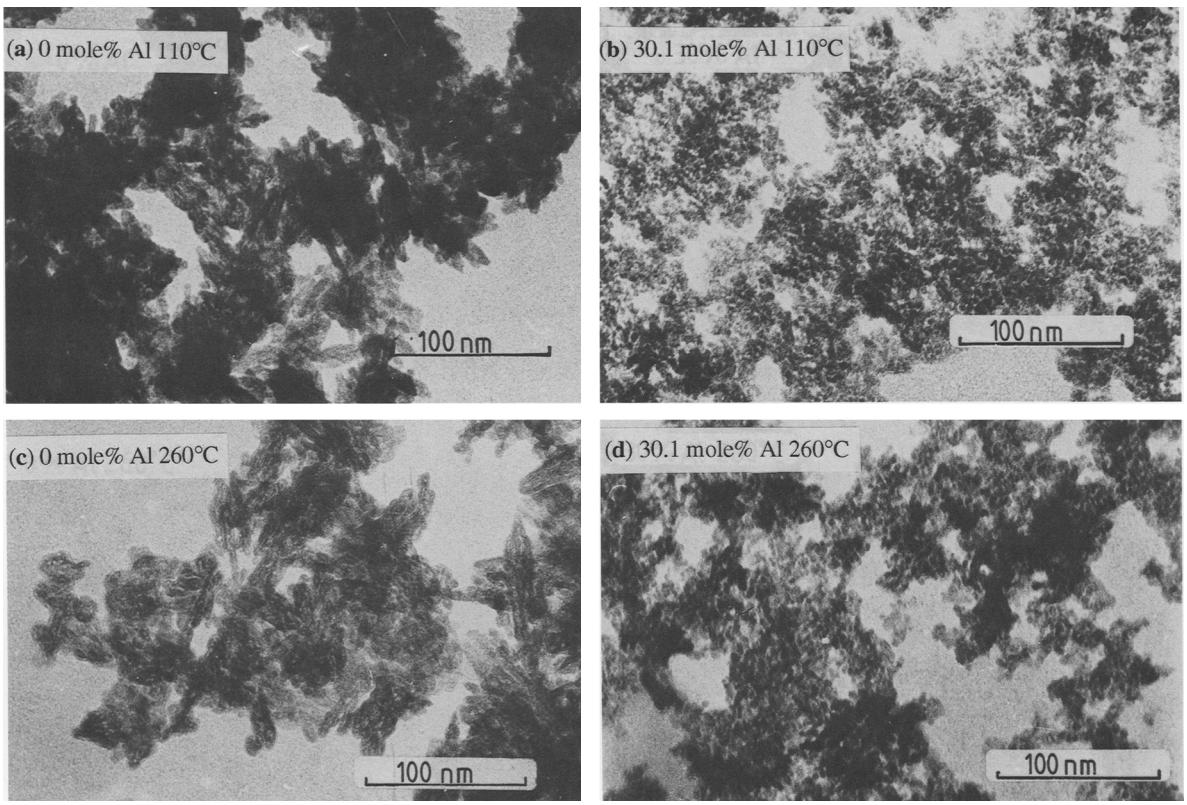

Figure 10. Transmission electron micrographs of goethite and corresponding hematite; (a) 0 mole % Al 110°C and (b) 30.1 mole% Al 110°C; (c) 0 mole % Al and (d) 30.1 mole% Al-substituted goethite heated at 260°C for one hour.

and particles of corresponding hematite, transformed from goethite at 260°C, inherited this crystal characteristic (Figures 10a and 10c). Goethite crystals decreased in size and altered to a more equant shape as Al-substitution increased (Figure 10b). These Al-goethites resemble those synthesized from the ferrous system by Fey and Dixon (1981) and Schulze (1982). There was no evident change in morphology associated with the dehydroxylation of goethite at low temperature (Figures 10c and 10d) but this may reflect the lack of resolution of the micrographs.

Mean coherence length (MCL) (i.e., size of coherently diffracting domains normal to hkl plane) for goethite and hematite determined by XRD line broadening are shown in Table 2. MCL values are mostly ~7 nm which compare well with MCL of synthetic goethites examined by Schulze (1982) and to particle sizes taken from the electron micrographs (Figure 10). For the samples heated at 110°C, MCL for Gt110 (i.e., goethite 110) and Gt111 reflections increased with Al-substitution levels from 0 to 9.7 mole % Al and then decreased between 9.7 and 30.1 mole % Al (Table 2). However, the MCL for the Gt020 and Gt151 reflections showed a decreasing trend as Al-substitution increased from 0 to 30.1 mole % (Table 2). The same trends were apparent for goethites heated at temperatures up to 210°C. These results indicate that crystals of non-substituted goethite are longer along the b axis (i.e., crystal width) than along the a axis (i.e., crystal thickness). In contrast, crystals of Al-substituted goethite are longer along the a axis than along the b axis (Table 2). There is no comparison of sizes along the c axis since no well resolved XRD line provides this information.

A schematic diagram illustrating the changes in crystal size and shape with Al-substitution and dehydroxylation to hematite is shown in Figure 11 and provides a succinct summary of the data. Fey and Dixon (1981) reported an increase in MCL with Al-substitution for the range 0 and 10 mole % Al and then a decrease between 10 and 40 mole % Al. Later, Schulze and Schwertmann (1987) indicated that MCL increased with Al-substitution over the range 0 and 20 mole % Al and then decreased between 20 and 33 mole % Al. Their results showed that goethite, with little or no Al-substitution, consisted of crystals with several coherently diffracting domains elongated along the c axis whereas at high level of Al substitution the crystals mainly consisted of monodomains. This trend is consistent with the data presented for the present investigation. MCL

https://doi.org/10.1346/CCMN.1995.0430207 Published online by Cambridge University Press

Table 2. The mean coherence length (nm) derived from XRD line broadening for goethite and hematite as affected by Al-substitution and heating.

	Reflection	Al (mole %)	Heating temperature (°C)										
			110	180	190	200	210	220	230	240	250	260	270
Gt	020	0	8.9	8.9	8.7	8.7	7.5						
		9.7	7.5	7.7	7.6	7.7	7.2						
		19.7	5.7	5.7	5.8	5.7	5.5	5.1					
		30.1	5.4	5.5	5.2	5.3	5.3	4.9					
	110	0	6.4	6.4	6.5	6.6	6.2	6.2					
		9.7	8.5	8.4	8.6	8.5	7.9	7.7	6.5				
		19.7	8.1	8.0	8.0	8.3	8.2	7.8	7.2				
		30.1	7.5	7.6	7.7	7.5	7.4	7.2	6.7	6.0			
	111	0	7.1	7.1	7.0	7.0	6.4						
		9.7	7.6	7.7	7.6	7.5	7.0	6.8					
		19.7	6.8	6.9	7.0	6.9	6.9	6.2					
		30.1	6.6	6.7	6.7	6.6	6.7	6.2					
	151	0	8.1	8.0	8.1	8.2	6.6						
		9.7	7.6	7.6	7.6	7.5	7.0	6.9					
		19.7	6.4	6.5	6.5	6.5	6.4	6.0					
		30.1	6.0	5.9	5.8	6.0	5.7	5.5					
Hm	102	0						4.6	4.9	5.0	5.2	5.4	5.7
		9.7							4.4	4.6	4.8	4.8	4.9
		19.7							3.0	4.1	4.1	4.2	4.3
		30.1								3.5	3.6	3.9	4.0
	110	0						6.7	10.0	10.5	10.9	11.2	11.8
		9.7							7.5	8.7	8.9	9.1	9.9
		19.7									5.8	7.0	7.7
		30.1									5.1	6.1	6.5
	204	0						6.7	6.7	6.9	7.1	7.2	7.5
		9.7							5.7	5.7	6.0	6.3	7.0
		19.7							5.0	5.6	5.7	5.8	6.0
		30.1								4.9	5.3	5.4	5.6
	116	0						7.8	8.2	8.8	9.3	9.5	10.8
		9.7							9.4	9.6	9.8	10.0	10.5
		19.7							8.8	9.3	9.3	9.3	9.3
		30.1								8.6	8.6	8.8	8.8

for goethites of the present study were unchanged by heating temperatures (i.e., <200°C) below which goethite started to transform to hematite and these results are consistent with those reported by Schwertmann *et al* (1985). Above this "threshold temperature" crystal size decreased. Conversely, MCL for the main reflections for hematite increased with increasing temperature. MCL of hematite decreased systematically with increasing Al-substitution (Table 2).

A comparison of crystal sizes derived from the 020 reflection (i.e., MCL Gt020) for goethite and the crystallographically equivalent hematite direction (MCL Hm110) are shown in Figure 12. There was a decrease in MCL Gt020 during decomposition of goethite (i.e., >200°C) and an increase in MCL of hematite (i.e., Hm110) during formation of hematite (Table 2; Figure 12a). The crystal size of goethite was smaller than that of the corresponding hematite that formed at temperatures greater than 250°C. The increase in crystal size with increasing temperature in the range from 230° to 270°C was greater for non-substituted hematite than for Al-hematite due at least partly to differences in dehydroxylation temperature (Table 2; Figure 12a). Although the size of newly-formed hematite crystals initially depended on the size of precursor goethite crystals or more precisely the size of domains in the b axis direction, the hematite domains expanded along the a axis with increasing temperature. The comparison of goethite MCL Gt110 and the closest equivalent hematite direction MCL Hm116 shows a similar trend with a reduction in size of goethite crystals above 200°C and the size of newly-formed hematite crystals increasing as heating temperature increased (Figure 12b). This increase in size reflects the growth of regularly ordered hematite domains by sintering and surface diffusion which induces coalescence of precursor goethite domains.

Specific surface area

Specific surface area of goethite increased linearly as Al-substitution increased (Figure 13a). The values of intercept and slope of regression lines for samples heated to 110°C are similar to the values calculated from the data of Fey and Dixon (1981) as is shown in Table

https://doi.org/10.1346/CCMN.1995.0430207 Published online by Cambridge University Press

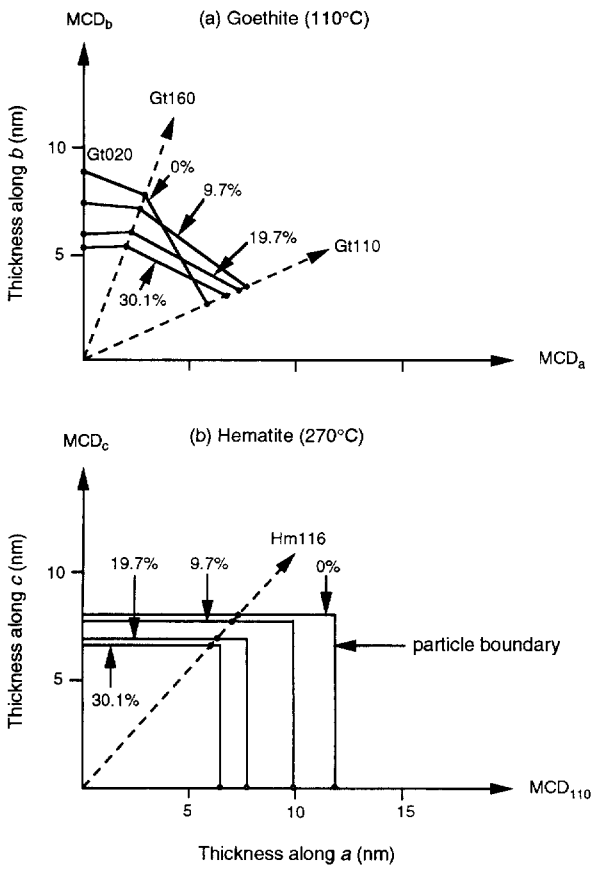

Figure 11. Polar diagram indicating the mean size and shape of goethite domains (a) in the (001) plane and of corresponding hematite crystallites (b) in the (010) plane. Dashed arrows indicate the directions normal to the lattice planes with the given Miller indices.

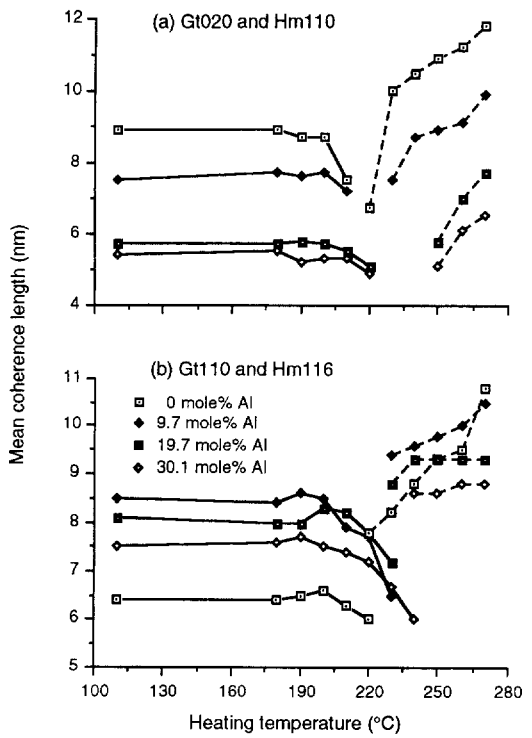

Figure 12. A comparison of mean coherence length (MCL) derived from XRD line broadening measurements of goethite and hematite reflections that approximately correspond to the same crystallographic directions; (a) Gt020 and Hm110, and (b) Gt110 and Hm116; plain lines for goethite and dashed lines for hematite.

3. The value of slope derived form the data of Goodman and Lewis (1981) is almost twice as large and the value of intercept is much smaller (Table 3). The increase in specific surface area is considered to be related to the decrease in goethite crystallite size with increase in Al-substitution. A moderate increase in specific surface area was induced by dehydroxylation to hematite due to the formation of pores (Watari *et al* 1979, 1983, Naono and Fujiwara 1980, Rendon *et al* 1983). Intercepts of plots of specific surface area versus Al-substitution (i.e., values for 0% Al-goethite heated between 110° and 260°C) increased from 143 to 184 m^2/g (Figure 13b) and the values of slope (rate of increase in specific surface area with increasing Al-substitution) decreased from 2.86 to 1.69 m^2/g/mole % Al (Figure 13c). The values of intercept increased up to 240°C and then decreased between 240° and 260°C (Figure 13b). This trend may predominantly reflect the development of slit-shaped microporosity during decomposition of goethite and formation of hematite at temperatures up to 240°C whereas between 240 and 260°C the processes of surface and volume diffusion may enable healing of crystal defects and the growth in size of hematite crystals with a consequent reduction in porosity (Watari *et al* 1979, 1983, Naono and Fujiwara 1980, Rendon *et al* 1983, Goss 1987). The rate of increase in specific surface area with Al-substitution (i.e., values of slope) decreased with temperature up to 240°C due predominantly to the smaller effect of heating on the surface area of high Al-substituted hematites (Figure 13c). These Al-hematites initially consisted of smaller particles of Al-goethite; thus loss of water during heating is less likely to generate voids as diffusion distances to crystal

Table 3. A comparison of intercept and slope values for specific surface area of goethites as affected by Al-substitution (heated at 70° or 110°C).

	Intercept (m^2/g)	Slope (m^2/g/ mole % Al)	$R^{2\,1}$
Present work	143	2.86	0.962*
Fey and Dixon (1981)	155	2.74	0.903*
Goodman and Lewis[2] (1981)	112	4.79	0.988**

[1] p (0.05*, 0.01**).
[2] Heated at 70°C.

https://doi.org/10.1346/CCMN.1995.0430207 Published online by Cambridge University Press

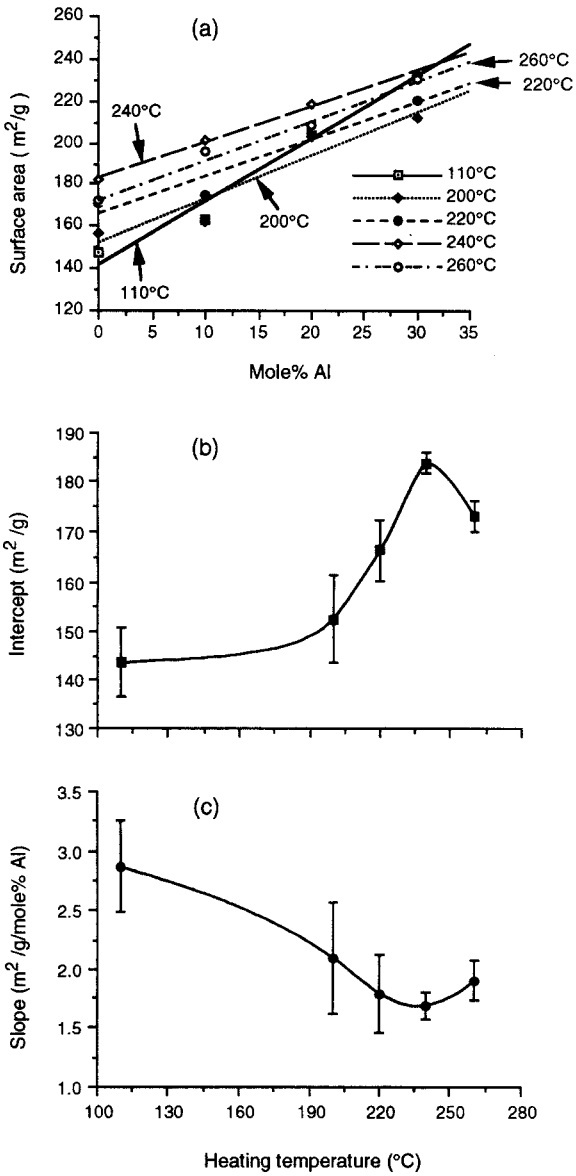

Figure 13. (a) Specific surface area of goethite as a function of Al-substitution for various heating temperatures, (110°C) y = 143 + 2.86x, R^2 = .96*, (200°C) y = 153 + 2.10x, R^2 = .90*, (220°C) y = 166 + 1.79x, R^2 = .92*, (240°C) y = 184 + 1.69x, R^2 = .98**, (260°C) y = 173 + 1.90x, R^2 = 0.98**, (*p < .05 and **p < .01, respectively); intercept (b) and slope (c) values for straight lines relating specific surface area to Al-substitution in goethite versus heating temperature.

surfaces are much smaller than in nonsubstituted hematite.

CONCLUSIONS

Al-substitution in goethite results in increases in dehydroxylation temperature and the amount of excess (non-stoichiometric) OH. Some of this excess OH is inherited by hematite formed by the dehydroxylation of goethite. The a dimension of goethite and the c dimension of hematite are enlarged and are the crystallographic axes that appear to be most sensitive to excess OH. The structural defects associated with an increase in pores which contributes to the increase in specific surface area may also disrupt Fe-O (Al-O) bonds thereby enabling excess structural OH to be retained during the thermal transformation of goethite to hematite.

The extent to which natural goethite and hematite in soils contain excess water has not been determined. The systematic changes in unit cell parameters of these minerals on heating to various temperatures that have been described in this paper may provide a basis for the investigation of the occurrence of excess OH in these naturally occurring iron oxides.

ACKNOWLEDGMENTS

The authors gratefully acknowledge Professor Dr. Udo Schwertmann and Dr. Helge Stanjek, of Technischen Universität München, Associate Professor Dr. Darrell G. Schulze, of Purdue University and Mr. Martin A. Wells, of the University of Western Australia, for their helpful advice on the manuscript.

REFERENCES

Anand, R. R., and R. J. Gilkes. 1984. Weathering of hornblende, plagioclase and chlorite in Meta-Dolerite Australia. *Geoderma* **34**: 261–280.

Bernal, J. D., D. R. Dasgupta, and A. L. Mackay. 1959. The oxides and hydroxides of iron and their structural interrelationships. *Clay Miner. Bulletin* **4**: 15–30.

Brown, G. 1980. *Crystal Structure of Clay Minerals and their X-ray Identification.* G. W. Brindley and G. Brown, eds. London: Mineralogical Society, pp. 361–410.

DeGrave, E., L. H. Bowen, and S. B. Weed. 1982. Mössbauer study of aluminum substituted hematites. *J. Magn. & Magn. Mat.* **72**: 129–140.

Fazey, P. G., B. H. O'Connor, and L. C. Hammond. 1991. X-Ray powder diffraction rietveld characterization of synthetic aluminum-substituted goethite. *Clays & Clay Miner.* **39**: 248–253.

Fey, M. B., and J. B. Dixon. 1981. Synthesis and properties of poorly crystalline hydrated aluminous goethites. *Clays & Clay Miner.* **29**: 91–100.

Francombe, M. H., and H. P. Rooksby. 1959. Structure transformations effected by the dehydration of diaspore, goethite and delta ferric oxide. *Clay Miner. Bulletin* **21**: 1–14.

Goodman, B. A., and D. G. Lewis. 1981. Mössbauer spectra of aluminous goethite (α-FeOOH). *J. Soil Sci.* **32**: 351–363.

Goss, C. J. 1987. The kinetics and reaction mechanism of the goethite to hematite transformation. *Miner. Mag.* **51**: 437–451.

Gregg, S. J., and K. J. Hill. 1953. The production of active solids by thermal decomposition. Part II. Ferric oxide. *J. Chem. Soc.* **IV**: 3945–3951.

Jónás, K., and K. Solymár. 1970. Preparation, X-ray, derivatographic and infrared study of aluminium-substituted goethites. *Acta Chim. Acad. Sci. Hung.* **66**: 383–394.

Lewis, D. G., and U. Schwertmann. 1979. The influence of Al on iron oxides. III. Preparation of Al-goethite in M KOH. *Clay Miner.* **14**: 115–126.

Lewis, D. G., and U. Schwertmann. 1980. The effect of [OH] on the goethite produced from ferrihydrite under alkaline conditions. *J. Colloid Interface Sci.* **78**: 543–553.

Lim-Nunez, R. S. L. 1985. Synthesis and acid dissolution of metal-substituted goethites and hematites: MSc. thesis. Department of Soil and Plant Nutrition, U.W.A., Nedlands, 6009, pp. 104–121.

Mackenzie, R. C., and G. Berggren. 1970. Oxides and hydroxides of higher valence elements. In *Differential Thermal Analysis 1*. R. C. Mackenzie, ed. New York: Academic Press, 271–302.

McKeague, J. A., and J. H. Day. 1966. Dithionite- and oxalate-extractable Fe and Al as aids in differentiating various classes of soils. *Can. J. Soil Sci.* **46**: 13–22.

Naono, H., and R. Fujiwara. 1980. Micropore formation due to thermal decomposition of acicular microcrystals of α-FeOOH. *J. Colloid Interface Sci.* **73**: 406–415.

Novak, G. A., and A. A. Colville. 1989. A practical interactive least-squares cell-parameter program using an electronic spreadsheet and a personal computer. *Amer. Miner.* **74**: 488–490.

Okamoto, G., R. Furuichi, and N. Sato. 1967. Chemical reactivity and electrical conductivity of hydrous ferric oxide. *Electrochim. Acta* **12**: 1287–1299.

Perinet, G., and R. Lafont. 1972a. Sur le paramétres cristallographiques des hématites aluminineuses. *C. R. Acad. Sci.* **275**: 1021–1024.

Perinet, G., and R. Lafont. 1972b. Sur la présence d'hématite aluminineuses désordonée dans des bauxites du Var. *C. R. Acad. Sci.* **274**: 272–274.

Rendon, J. L., J. Cornejo, P. Dearambarri, and C. J. Serna. 1983. Pore structure of thermally treated goethite (α-FeOOH). *J. Colloid Interface Sci.* **92**: 508–516.

Schulze, D. G. 1982. The identification of iron oxides by differential X-ray diffraction and the influence of aluminum substitution on the structure of goethite: Ph.D. thesis. Lehrstuhl für Bodenkunde der Technischen Universität München, Weihenstephan.

Schulze, D. G. 1984. The influence of aluminum on iron oxides. VIII. Unit-cell dimensions of Al-substituted goethites and estimation of Al from them. *Clay & Clay Miner.* **32**: 36–44.

Schulze, D. G., and U. Schwertmann. 1984. The influence of aluminium on iron oxides: X. Properties of Al-substituted goethites. *Clay Miner.* **19**: 521–539.

Schulze, D. G., and U. Schwertmann. 1987. The influence of aluminium on iron oxides: XIII. Properties of goethites synthesised in 0.3 M KOH at 25°C. *Clay Miner.* **22**: 83–92.

Schwertmann, U., P. Cambier, and E. Murad. 1985. Properties of goethites of varying crystallinity. *Clays & Clay Miner.* **33**: 369–378.

Schwertmann, U., R. W. Fitzpatrick, R. M. Taylor, and D. G. Lewis. 1979. The influence of aluminium on iron oxides. Part II. Preparation and properties of Al-substituted hematites. *Clays & Clay Miner.* **27**: 105–112.

Singh, B., and R. J. Gilkes. 1992. XPAS: An interactive computer program for analysis of X-ray powder diffraction patterns. *Powder Diffraction* **7**: 6–10.

Stanjek, H., and U. Schwertmann. 1992. The influence of aluminium on iron oxides. Part XVI: Hydroxyl and aluminium substitution in synthetic hematites. *Clays & Clay Miner.* **40**: 347–354.

Taylor, M. R., and U. Schwertmann. 1978. The influence of aluminium on iron oxides. Part I. The influence of Al on Fe oxide formation from the Fe (II) system. *Clays & Clay Miner.* **26**: 373–383.

Thiel, R. 1963. Zum system α-FeOOH-α-AlOOH. *Z. Anorg. Allg. Chem.* **326**: 70–78.

Watari, F., J. van Landuyt, P. Delavignette, and S. Amelinckx. 1979. Electron microscopic study of dehydration transformations I. Twin formation and mosaic structure in hematite derived from goethite. *J. Solid State Chem.* **29**: 137–150.

Watari, F., P. Delavignette, J. van Landuyt, and S. Amelinckx. 1983. Electron microscopic study of dehydration transformations III. High resolution observation of the reaction process FeOOH → Fe_2O_3. *J. Solid State Chem.* **48**: 49–64.

Wells, M. A., R. J. Gilkes, and R. R. Anand. 1989. The formation of corundum and aluminous hematite by the thermal dehydroxylation of aluminous goethite. *Clay Miner.* **24**: 513–530.

Wolska, E., 1981. The structure of hydrohematite. *Z. Kristallographie* **154**: 69–75.

Wolska, E., and U. Schwertmann. 1989. Nonstoichiometric structures during dehydroxylation of goethite. *Z. Kristallographie* **189**: 223–237.

Wolska, E., and W. Szajda. 1985. Structural and spectroscopic characteristics of synthetic hydrohematite. *J. Mater. Sci.* **20**: 4407–4412.

(Received 11 February 1994; accepted 27 September 1994; Ms. 2469)